

EFFECT OF STRAIN RATE AT COMPRESSIVE AND TENSILE LOADING OF UNIDIRECTIONAL PLYS IN STRUCTURAL COMPOSITES

V.Singh^{1,2*}, R. Larsson², E. Marklund¹, R. Olsson^{1,2}

¹ RISE Research Institutes of Sweden, Division of Materials and Production
RISE SICOMP AB, Box 104, SE-431 22 Mölndal, Sweden

² Div. Material & Computational Mechanics, Chalmers University of Technology

* vivekendra.singh@ri.se

Key words: Constitutive model, Strain rate effects, Unidirectional composites.

Summary: *Fibre-reinforced polymer composites are widely used in structural applications due to their high specific stiffness and strength. In some applications the response of dynamically loaded composite components must be analysed. For example, in crash analyses of structural components, where very high loading rates occurs, the composite behaviour is not fully understood. For this, we present a novel transversely isotropic viscoelastic-viscoplastic constitutive model for a unidirectional carbon-epoxy composite. The model is micromechanically motivated so that the matrix and fibre materials of the composite are treated as micromechanical constituents at the ply scale. Based on the Hill-Mandel condition, the phases are homogenized via the macroscopic and fluctuating strain fields. To arrive at a simple but still representative model, a simplistic ansatz is applied to the structure of the fluctuating strains leading to a non-standard homogenized response of the composite. The model is applied to the non-linear rate dependent anisotropic ply behaviour under quasi-static and dynamic loading at different off-axis angles. For a simple viscoelastic-viscoplastic prototype for the rate dependent matrix response, there is a good correlation between measured and model response of the IM7-8552 material system in compression and tension.*

1 INTRODUCTION

For the last few decades, laminated fibre reinforced polymer (FRP) composites have been implemented in aerospace and automotive applications due to their high specific stiffness, strength and ability to be tailored as per the application which makes them exceedingly attractive when compared with conventional materials. However, certain technological applications are frequently subjected to dynamic loads such as automotive crash, where the load is applied dynamically, resulting in the development of high rates of strain and stress. These scenarios cannot be designed or modelled with static properties, which might be too conservative to consider. The main reason is that mechanical properties of composites vary significantly with the strain rate.

Therefore, it is necessary to understand the behaviour of the composites at different strain rates. It has been reported in many experimental studies that the strain rate influences the mechanical properties of composites, but the level of sensitivity depends on material system constituents.

It has been experimentally proven that carbon fibres are strain rate insensitive, while e.g. glass and Kevlar® (aramid) fibres are strain rate sensitive. It was also found that mechanical properties of pure resins are strain rate sensitive [4]. For this reason, longitudinal tensile properties of unidirectional carbon/epoxy laminates are virtually strain rate insensitive. Moderate rate effects were however reported for the transverse and interlaminar tensile properties. The compressive properties of unidirectional polymer composites experience a significant strain rate effect in longitudinal, transverse and shear direction [4].

Therefore, based on the above observations, it is required to develop an advanced composite material model to simulate strain rate effects and non-linear stress-strain behaviour of the dynamic response of polymer composites relevant for several loading scenarios such as bird impact and automobile crash. The objective of this paper is to present a novel fully three-dimensional micro mechanically motivated transversely isotropic viscoelastic-viscoplastic constitutive model for a unidirectional (UD) carbon-epoxy composite, which can capture the strain rate dependent behaviour of a UD composite in tension, compression and shear. The model applies to the ply scale and it is based on a structural tensor-based formulation along the lines set out in [1] for the representation of off-axis compression/extension of the composite. The model is validated and calibrated with the already available off-axis and transverse compression and tension test data for IM7-8552 presented in [2,3].

2 HOMOGENIZED RESPONSE OF THE MATRIX-FIBRE COMPOSITE

Consider a Representative Volume Element (RVE) B_{\square} of the fibre/matrix composite as shown in Figure 1. The matrix material is in the region B_{\square}^m and the fibre material is in the region B_{\square}^f . Consider also the microscopic strain field $\boldsymbol{\varepsilon} \in B_{\square}$ split into a macroscopic, constant (average) strain $\bar{\boldsymbol{\varepsilon}} = (\bar{\mathbf{u}} \otimes \nabla)^{sym}$ in the RVE (where $\bar{\mathbf{u}}$ is the macroscopic displacement of the solid), and a fluctuating portion $\tilde{\boldsymbol{\varepsilon}} \in B_{\square}$. The total strain in B_{\square} is thus obtained as

$$\boldsymbol{\varepsilon} = \bar{\boldsymbol{\varepsilon}} + \tilde{\boldsymbol{\varepsilon}} \quad (1)$$

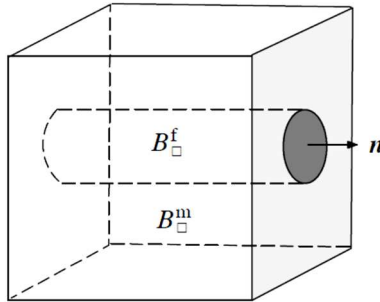


Figure 1 : Representative volume element of composite with volume V_{\square} with a fibre region $B_{\square}^f \in B_{\square}$ (with the fibre orientation \mathbf{n}) embedded in the polymer matrix $B_{\square}^m \in B_{\square}$. In the different regions it is assumed that the micro-stresses $\boldsymbol{\sigma}^m \in B_{\square}^m$ and $\boldsymbol{\sigma}^f \in B_{\square}^f$ are constant.

In order to derive the homogenized response of the deformation process in the RVE, let us exploit the principle of virtual work equivalence applied to the representative region B_{\square} in Figure. 1, cf. e.g. refs. [5,6]. To arrive at a simplistic but still representative homogenized response of the composite, it is noted that constant strain in the fibre direction is acceptable, even in the non-linear regime of the micro-mechanical response. In the transverse direction of the fibre it is rather the stress that is constant across the constituents, whereby the fluctuation

$\tilde{\boldsymbol{\varepsilon}}$ is most significant with respect to the transverse direction of the fibre. To formulate this, it is assumed (as is also suggested in the figure 1) that the stress and strain fields are piecewise constant in B_{\square} so that

$$\tilde{\boldsymbol{\varepsilon}} = \begin{cases} \tilde{\boldsymbol{\varepsilon}}^m & \boldsymbol{x} \in B_{\square}^m \\ \tilde{\boldsymbol{\varepsilon}}^f & \boldsymbol{x} \in B_{\square}^f \end{cases}, \boldsymbol{\sigma} = \begin{cases} \boldsymbol{\sigma}^m & \boldsymbol{x} \in B_{\square}^m \\ \boldsymbol{\sigma}^f & \boldsymbol{x} \in B_{\square}^f \end{cases} \quad (2)$$

where $\tilde{\boldsymbol{\varepsilon}}^m$ and $\tilde{\boldsymbol{\varepsilon}}^f$ are the fluctuations in matrix and fibre. To allow for that the micro stress in B_{\square} is constant in the transverse fibre direction, we choose $\tilde{\boldsymbol{\varepsilon}}^m = b\hat{\boldsymbol{\varepsilon}}$ where b is a scalar variable of the strain fluctuation and $\hat{\boldsymbol{\varepsilon}}$ is the projected *macroscopic* strain tensor onto the transverse direction of the fibre. This tensor is defined in terms of the second order isotropy plane identity tensor $\hat{\mathbf{1}}$ as

$$\hat{\boldsymbol{\varepsilon}} = (\boldsymbol{\varepsilon} \cdot \hat{\mathbf{1}})^{sym} = \hat{\mathbf{I}} : \boldsymbol{\varepsilon} \quad \text{with} \quad \hat{\mathbf{I}} = \frac{1}{2} (\hat{\mathbf{1}} \otimes \hat{\mathbf{1}} + \mathbf{1} \otimes \hat{\mathbf{1}}) \quad (3)$$

with $\hat{\mathbf{1}} = \mathbf{1} - \boldsymbol{a}$ where $\mathbf{1}$ is the second order identity tensor and $\boldsymbol{a} = \boldsymbol{n} \otimes \boldsymbol{n}$ is the structure tensor normal to the fibre face where \boldsymbol{n} is the unit normal vector as shown in Fig. 1. Moreover, $\hat{\mathbf{I}}$ is the 4th order fibre transverse projection operator. Upon inserting these expressions into the Hill-Mandel condition, it appears that the consistent homogenized macroscopic stress is obtained as

$$\bar{\boldsymbol{\sigma}} = \left((1 - v^f) \boldsymbol{\sigma}^m + v^f \boldsymbol{\sigma}^f \right) : (\mathbf{I} + b\hat{\mathbf{I}}) - b\boldsymbol{\sigma}^f : \hat{\mathbf{I}} \quad (4)$$

corresponding to the continuity relation $(\boldsymbol{\sigma}^m - \boldsymbol{\sigma}^f) : \hat{\boldsymbol{\varepsilon}} = 0$ in the intrinsic matrix and fibre stresses $\boldsymbol{\sigma}^m$ and $\boldsymbol{\sigma}^f$, respectively. As desired from the outset, the intrinsic matrix and fibre stresses balance each other so that these stresses are continuous in the transverse fibre straining direction $\hat{\boldsymbol{\varepsilon}}$. Moreover, in (4) v^f is the fibre volume fraction.

To account for the directional influence of the fibres in the composite a Voigt model (constant strain) was used in the direction of the fibres and a Reuss model (constant stress) was used in the direction transverse to the fibres.

3 MODELING OF THE POLYMER MATRIX AND THE FIBRE MATERIAL

To model the intrinsic *polymer matrix*, it is assumed that the ‘‘elastic’’ shear response of the polymer matrix material is linearly viscoelastic combined with a viscoplastic deformation mechanism. For this, consider the rheological model in Figure. 2 for the viscoelastic-viscoplastic coupling. This coupling is described in terms of the ‘‘static’’ shear modulus G_1 and the dynamic shear stiffness $G_{\infty} = G_1 + G_2$, representing the elastic response at very high loading rates (when the visco-elastic damper has no time to develop viscous deformation). As to viscoplasticity, the damper starts to develop inelastic deformation as soon as the slider starts to open as defined in terms of an over stress function, cf. Figure. 2.

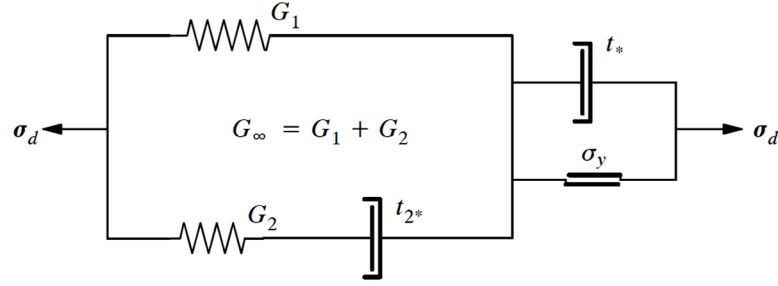


Figure 2: Rheological model for the in-elastic response of the matrix of the composite. It consists of a viscoelastic 3 parameter response combined with a viscoplastic deformation mechanism.

This corresponds to the total matrix stress $\boldsymbol{\sigma}^m = \boldsymbol{\sigma}_d^m + \sigma_v^m \mathbf{1}$, where subscript “ d ” refers to the deviatoric and “ v ” to the volumetric component and the constitutive state equations are

$$\boldsymbol{\sigma}_d^m = 2G_1(\boldsymbol{\varepsilon}_d - \boldsymbol{\varepsilon}_d^p) + 2G_2(\boldsymbol{\varepsilon}_d - \boldsymbol{\varepsilon}_d^p - \boldsymbol{\varepsilon}_d^v) \quad (5)$$

$$\sigma_v^m = K_v^m \varepsilon_v, \quad \varepsilon_v = \mathbf{1} : \boldsymbol{\varepsilon} \quad (6)$$

where $\boldsymbol{\varepsilon}_d$ and ε_v are deviatoric and volumetric strain, whereas $\boldsymbol{\sigma}_d^m$ and σ_v^m are deviatoric and volumetric matrix stresses. K_v^m is the elastic bulk modulus of the polymer. Moreover, $\boldsymbol{\varepsilon}_d^v$ is the deviatoric in-elastic viscous portion of the strain. The viscoplastic strain $\boldsymbol{\varepsilon}_d^p$ is involved in the elastic deviatoric strain defined by $\boldsymbol{\varepsilon}_d^e = \boldsymbol{\varepsilon}_d - \boldsymbol{\varepsilon}_d^p$. We introduce the viscoplastic/viscoelastic evolution rules related to the matrix shear behaviour defined as

$$\dot{\boldsymbol{\varepsilon}}_d^p = \lambda \mathbf{f} \text{ with } \mathbf{f} = \frac{3}{2} \frac{\boldsymbol{\sigma}_d^m}{\sigma_d^e} \text{ and } \dot{\boldsymbol{\varepsilon}}_d^v = \frac{1}{2G_2 t_{2*}} \boldsymbol{\sigma}_{d2}^m \quad (7)$$

where $\sigma_d^e = 3/2|\boldsymbol{\sigma}_d^m|$ is the effective von Mises stress of the matrix and t_{2*} is the relaxation time parameter of the elastic viscous damper. To describe the viscoplastic creep response, a Bingham creep model is employed in terms of the viscoplastic multiplier λ and the yield function ϕ defined as:

$$\lambda = \frac{1}{t_*} \eta \text{ with } \eta = \frac{\langle \sigma_d^e - \sigma_y - \gamma p \rangle}{3G_\infty} \quad (8)$$

where t_* is the viscoplastic relaxation time and η is the overstress function of Bingham type. $p = -\sigma_v^m$ is the matrix pressure. Moreover, γ is the friction parameter.

The *carbon fibre material* of the UD-composite is assumed *elastic* transversely isotropic. We have for the intrinsic fibre stress that $\boldsymbol{\sigma}^f = \boldsymbol{\sigma}_d^f + \sigma_v^f \mathbf{1} + \boldsymbol{\sigma}_s^f + \sigma_n^f \mathbf{a}$, where the individual stress contributions are

$$\boldsymbol{\sigma}_d^f = 2G_d^f \boldsymbol{\varepsilon}_d, \quad \boldsymbol{\sigma}_s^f = 2G_s^f \boldsymbol{\varepsilon}_s, \quad \sigma_v^f = K_v^f \varepsilon_v + \frac{\nu^f}{1 - \nu^f} E^f \varepsilon_n \quad (9)$$

$$\sigma_n^f = E^f \varepsilon_n, \quad \varepsilon_n = \mathbf{a} : \boldsymbol{\varepsilon} \quad (10)$$

where G_d^f is the shear modulus of the fibre and K_v^f is the bulk modulus of the fibre. $\boldsymbol{\sigma}_s^f$ and σ_n^f

are longitudinal shear and normal fibre stresses whereas, ε_n is the longitudinal normal fibre strain tensor and ε_s is the fibre shear strain tensor, cf. ref [1]. Moreover, E^f is the longitudinal fibre modulus of elasticity and ν^f is the Poisson's ratio when considering the fibre as isotropic in the fibre direction.

4 RESULTS

4.1 Material data and calibration of the model parameters

In this subsection, the material parameters and the calibration of the model parameters are briefly discussed. The assumed material parameters for the fibre and matrix are given in Table 1 and Table 2. The conversion to the corresponding parameters used in the present structure tensor representation is made as in ref. [1].

Table 1: Material parameters for the fibre.

E_1^f (GPa)	E_2^f (GPa)	G_{12}^f (GPa)	G_{23}^f (GPa)	K_v^f (GPa)	ν_{12}^f	ν_{23}^f
276	27	30	9.0	24.6	0.25	0.5

Table 2: Material parameters for the matrix.

E^m (GPa)	$G_1 = G^m$ (GPa)	K^m (GPa)	ν^m
3	1.1	3.5	0.36

To calibrate the model parameters, the axial stress-strain curves from the 45° off-axis compression tests are used. These tests were performed at quasi-static strain rate of $4 \cdot 10^{-4}$ /s and dynamic axial strain rates of 246 /s and 321 /s for compression loading and 177 /s and 300 /s for tensile loading.

The viscoelastic behaviour is calibrated using only three scalar parameters, G_1 , G_2 and t_{2*} of the generalized Maxwell model. Out of them only two scalar parameters are needed to be calibrated G_2 and t_{2*} due to the fact that G_1 is a physical parameter defined as the static shear modulus of a matrix. In addition to that the evolution equation for the viscous strain is independent of the hydrostatic pressure. Hence, viscoelastic behaviour is similar in both tension and compression loading.

Table 3: Calibrated viscoelastic-viscoplastic model parameters for the matrix material.

G_2 (GPa)	t_{2*}	σ_y (MPa)	t_*
0.81	14.26	194	0.11

The viscoplastic behaviour is fully determined using the scalar parameters, σ_y , t_* and γ . The pressure dependence of the onset of plastic yielding in matrix shear dominated response under compressive loading of the ply has also been considered in the model. However, it was found that the model calibration results are in good agreement without considering hydrostatic pressure with experimental data under uniaxial compression loading. Therefore, only two scalar parameters σ_y and t_* are used to calibrate viscoplastic behaviour. The calibrated model parameters which give the best approximation are listed in Table 3.

4.2 Compression and tension results

Figures 3 and 4 show the measured [2,3] and simulated static and dynamic axial stress-strain curves under 45° and 30° off-axis tension and compression. The dotted line refers to the experimental results, the continuous line refers to the simulation results. A good prediction of the nonlinear behaviour could be achieved, both for quasi-static and dynamic loading.

It can be seen by considering the experimental data of the static and dynamic 30°, 45°, 60° and 75° off-axis tensile and compression tests that the stiffness increases with increasing strain rate in the elastic range and the axial stress-strain curves become more linear under dynamic loading. That means that viscous effects play a significant role not only in the elastic range, but also in the plastic range. With the viscoelastic-viscoplastic material model presented in this work, however, viscous effects are accurately predicted by the presented model.

It is also worth mentioning that the model parameters calibrated from the 45° off-axis compression test are used to simulate other off-axis compression and tension experimental tests and results are in good agreement with test data.

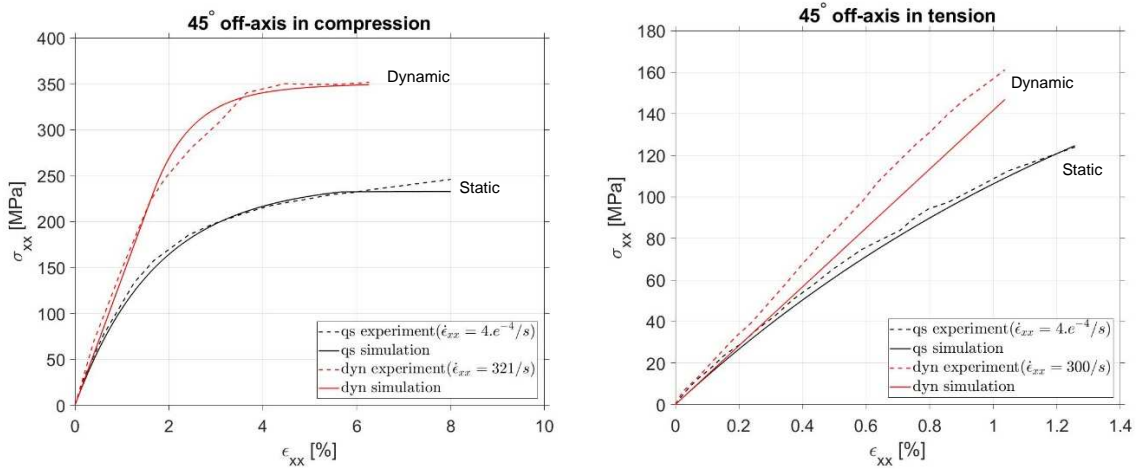


Figure 3: Quasi-static and dynamic axial stress-strain curves for the experiment and simulation of 45° off-axis in compression and tension [2,3]

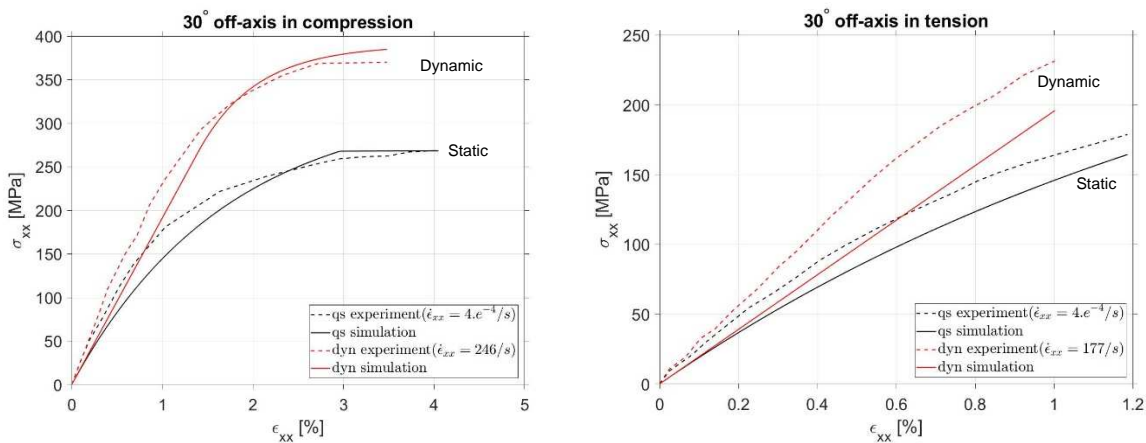


Figure 4: Quasi-static and dynamic axial stress-strain curves for the experiment and simulation of 30° off-axis in compression and tension [2,3]

5 CONCLUSIONS

A three-dimensional transversely isotropic viscoelastic-viscoplastic constitutive model at the ply scale, is presented. The model is focusing on the matrix shear dominated response under compressive and tensile loading of the ply. The current version considers damage growth indirectly through viscoplasticity but does not contain a damage parameter or any criteria for final failure. The model can be used with any orientation since it is a structure tensor based formulation. Furthermore, viscous effects are included in the modeling of the elastic and plastic regions and the model predicts the stress state in a specimen at high strain rate regimes with a reasonable accuracy. It might be possible to get even more realistic results with more complex homogenization such as the Mori-Tanaka model or various self-consistent techniques. Still the challenge would be how to efficiently implement them for simulating the non-linear regime of the micro-mechanical response.

The development of a strain rate dependent failure criterion considering strength and fracture toughness coupled with a viscoelastic-viscoplastic constitutive model will be addressed in future work.

6 ACKNOWLEDGEMENTS

The first author gratefully acknowledges the support of the ICONIC project under the Marie Skłodowska-Curie grant agreement No 721256 of the European Union Horizon 2020 research and innovation programme

REFERENCES

- [1] R. Larsson, R. Gutkin, S. Rouhi, Damage growth and strain localization in compressive loaded fiber reinforced composites. *Mechanics of Materials*, **127**, 77 – 90, 2018.
- [2] H. Koerber, J. Xavier, P.P. Camanho, High strain rate characterisation of unidirectional loaded fiber reinforced carbon-epoxy IM7-8552 in transverse compression and in-plane shear using digital image correlation. *Mechanics of Materials*, **42**, 1004-1019, 2010.
- [3] P. Kuhn, M. Ploeckl, and H. Koerber, Experimental investigation of the failure envelope of unidirectional carbon-epoxy composite under high strain rate transverse and off-axis tensile loading. *EPJ Web of Conferences*, **94**, 01040, 2015.
- [4] V. Singh, Literature survey of strain rate effects on composites, *Technical report*, TR18-001, Swerea SICOMP, Mölndal, 2018.
- [5] P. Suquet, *Local and global aspects in the mathematical theory of plasticity*, In A. Sawczuk, and G. Bianchi, editors, *Plasticity today: modelling, methods and applications*, pp. 279-310, London. Elsevier Applied Science Publishers, 1985.
- [6] C. Miehe, J. Schroder, J. Schotte, Computational homogenization analysis in finite plasticity. simulation of texture development in poly- crystalline materials. *Computer Methods in Applied Mechanics and Engineering*, **171**, 387–418, 1999.